A Simple Method for High-Quality Ultra-Thin Graphene Oxide Films Facilitates Nanoscale Investigations of Ion and Water Adsorption

*Raju R. Kumal, Amanda J. Carr, and Ahmet Uysal**

Chemical Sciences and Engineering Division, Argonne National Laboratory, Lemont, IL 60439, United States

Graphene oxide (GO) is a promising material for separations. Nanoscale GO thin films at the air/water interface are excellent experimental models to understand molecular-scale interactions of ions and water with GO. However, thin film formation strongly depends on how the GO was processed. This paper reports a simple, reliable, and quick method of preparing ultra-thin GO films, irrespective of their origin. This method allows the quantitative investigation of differences in film structure, ion adsorption, and interfacial water behavior with multiple surface sensitive probes. The data show that functional groups and oxidative debris vary significantly between different commercially available GO samples. These differences strongly affect ion adsorption and interfacial water behavior near GO, which are vital properties in separation applications. The results demonstrate the importance of the GO process conditions and provide experimental methods to quantify molecular-scale differences between different GO films.

Graphene oxide (GO) is a promising separation material because it combines molecular sieving with high water permeation.[1-5] The hydrophobic and hydrophilic patches on GO and their molecular-scale distribution can significantly alter mass transport.[6, 7] However, direct observation of water structure near GO surfaces is very difficult in real membrane applications. Therefore, large area, ultra-thin GO films with thicknesses of only a few nanometers are vital model systems that can be easily compared to computational studies.[8] The amphiphilic nature of GO has been exploited to create Langmuir films at the air/water interface.[9-12] These films can be transferred on solid substrates or studied directly at the liquid surface. However, there are multiple factors that affect GO thin film formation that are often overlooked, which leads to inconsistencies between reported studies. First, the chemical composition of the GO, including the number and types of functional groups as well as the flake size distribution, strongly depends on the specific synthetic procedure. Second, thin films are created at the air/water interface by preparing and spreading a dilute solution of GO (typically in a methanol/water mixture). This paper introduces a simple and effective spreading process. The prepared films are high quality, i.e. homogeneous across macro dimensions and smooth, and can be examined with surface-specific probes to reveal molecular-scale details including information about ion adsorption and interfacial water structure.

GO is not a perfect amphiphile in contrast to lipids with distinct hydrophobic tails and hydrophilic heads. Therefore, during the Langmuir film formation a significant amount of GO dissolves in the water subphase while only a small amount of material forms the thin film at the interface. Dissolution of GO in the subphase has been acknowledged since early investigations.[10] To promote interfacial film formation, studies have suggested options such as sonicating the GO spreading solution to disperse flakes,[13] introducing additional surfactants,[14] bubbling nitrogen through the subphase to transport GO flakes to the surface,[15] or decreasing the droplet size of the

GO spreading solution through electro-spraying.[16] The latter two options require additional equipment. All of these methods also utilized large volumes of the GO spreading solution (typically 1-10 mL of 0.2 mg/mL GO solution) to create ~100 cm^2 thin films. Spreading these large volumes via dropwise addition on a subphase can take up to 30 minutes.

Several studies are focused on the *in situ* characterization of GO films at the air/water interface. Bonatout et al. used X-ray reflectivity (XR) and suggested a bilayer structure for GO sheets with water molecule bridges.[13] This study did not report the amount of spreading solution used. The maximum momentum transfer, q_{max}, for XR data was 0.35 $Å^{-1}$, which suggests a rough surface and limits their resolution to $\frac{\pi}{q_{max}} \sim 9$ Å. The study also did not show the calculated electron density profiles from the XR fits but reported the fit parameters for a two-layer model, which suggests a 2 nm total thickness for the GO film. López-Díaz et al. used neutron reflectivity (NR) to show that the oxidative debris can form an extra layer underneath GO films.[17] They used a two-layer model to fit the NR data, with 2 nm GO and 1 nm impurity layer. The purified samples showed a single 2 nm GO layer. This study used 2.5 mL of spreading solution. The q_{max} of NR data was 0.2 $Å^{-1}$, meaning their resolution was 16 Å. These studies only focused on the GO structure and did not investigate ion or water interactions with the GO film. Hong et al. studied the structure of water near GO using vibrational sum frequency generation (VSFG) spectroscopy.[11] They used 1.1 mL spreading solution. VSFG does not provide direct structural information about the GO films. Instead, it provides the structure of interfacial water and its response to the salts in the subphase.[11] Recently, Carr et al. investigated monovalent, divalent, and trivalent ion adsorption on GO films using XR and VSFG.[18] The q_{max} for the XR data was 0.55 $Å^{-1}$, which gives a resolution of 6 Å. The spreading solution volume was 1 mL.

This work reports a simple and effective method to prepare GO films at the air/water interface by sonicating and filtering the GO spreading solution, which is then placed on a subphase via dropwise addition with a micro syringe (Figure 1). This process decreases the total GO spreading volume to ~100 μL, a 10 - 100x improvement versus prior studies, thus significantly reducing GO dissolution and decreasing the thin film prep time to a few minutes. The resulting films are high quality, i.e. very smooth and uniform, and allow XR measurements up to $q_{max} = 0.7$ $Å^{-1}$, which gives the highest resolution (4.5 Å) XR data on GO films at the air/water interface to date. The high quality of the GO films also facilitates observation of a new water population, via VSFG, that primarily interacts with the GO film. This water population has not been observed in previous studies at the air/water interface.[11, 18]

To demonstrate the universality of the preparation method, three commercially obtained GO samples were compared: 1 mg/mL GO (Sigma Aldrich, USA) (GO-1), 1 mg/mL carboxyl-enriched GO (Sigma Aldrich, USA) (GO-2), and 10 mg/mL GO diluted to 1 mg/mL with ultrapure water (Standard Graphene, South Korea) (GO-3). The carbon/oxygen ratios of each sample were 1.09, 1.55, and 1.21 for GO-1, GO-2, and GO-3, respectively, as determined using X-ray photoelectron spectroscopy (XPS) (Supporting Information). Each GO solution was diluted in a methanol/water (5:1, v/v) mixture to get a final concentration of 0.17 mg/mL. Samples were then sonicated for 1 hour and filtered with a 1.2 μm syringe filter (Figure 1b). The final solution is slightly lighter in color than the original 1 mg/mL stock solutions. The sonicated and filtered samples are labeled GO-1a, GO-2a, and GO-3a, and the untreated samples, which are neither sonicated nor filtered, are labeled as GO-1b, GO-2b, and GO-3b (Figure 1).

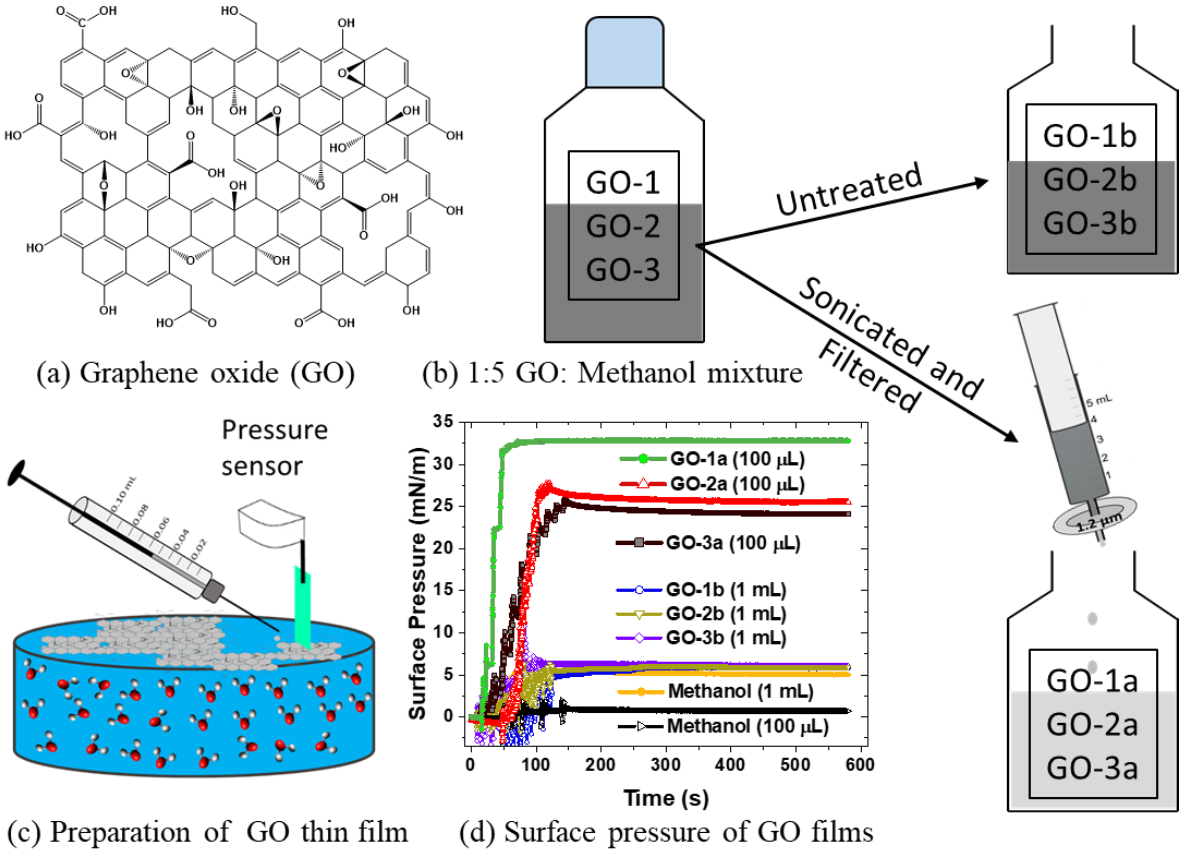

(a) Graphene oxide (GO) (b) 1:5 GO: Methanol mixture

(c) Preparation of GO thin film (d) Surface pressure of GO films

Figure 1. (a) Representative structure of the graphene oxide (GO). (b) 1 mg/mL aqueous GO suspensions (GO-1, GO-2, and GO-3) are diluted with a methanol/water mixture (1:5, v/v). Samples were then sonicated for an hour and filtered using a 1.2 µm syringe filter to create GO-1a, GO-2a, and GO-3a. Untreated samples are labelled as GO-1b, GO-2b, and GO-3b. (c) GO thin films were prepared in a PTFE dish by spreading 100 µL of GO spreading solution. The surface pressure was measured using a NIMA pressure sensor with a chromatography paper as a Wilhelmy plate. (d) Surface pressure of different GO samples and pure methanol at the air/water interface over time.

There are two key steps in this preparation process. First, sonication is completed in the methanol/water mixture. Sonicating only in water does not yield high quality films (data not shown). Second, samples were filtered after sonication. Samples that were sonicated but not filtered did not form good quality films (Supporting Information Figure SI2). It reasons that filtering removes any remaining GO aggregates, which prevents the suspended flakes from stacking and allows the flakes to float on the subphase. Both sonication and filtration had been used in previous studies.[11, 13, 17, 18] However, the relatively longer sonication reported here followed by filtering (1.2 μm filter) decreases the amount of spreading solution by 10 - 100x and forms significantly smoother films, which allows highly sensitive measurements.

Figure 1c shows a GO thin film formed in a fixed area by spreading the GO solution with a micro syringe. Figure 1d shows the measured surface pressure as a function of time during spreading for each solution. Spreading is completed in 100 seconds. The sonicated and filtered samples (GO-1a, GO-2a, GO-3a) reach a high surface pressure after 100 μL solution is spread. GO-2a and GO-3a show a similar trend while GO-1a reaches a higher surface pressure, which will be discussed below. The untreated samples (GO-1b, GO-2b, GO-3b) show very small changes in surface pressure even after ten times more (1 mL) spreading solution was used. Indeed, a control experiment with only 1 mL methanol shows a similar change in the surface pressure, which suggests that the untreated GO does not have a significant presence at the interface. GO films were also prepared in a Langmuir trough by spreading the GO solution over a larger area and then compressing the barrier to reach a surface pressure of 20 mN/m. These films are used in synchrotron X-ray experiments.

Figure 2 shows the VSFG data from -OH and -CH regions of the GO films. The equation used to model the data and the obtained fit parameters are given in the Supporting Information.

All of the high quality films (GO-1a, GO-2a, and GO-3a) show a strong water band with three peaks centered at 3250, 3440, and 3640 cm^{-1}. The 3250 and 3440 cm^{-1} peaks are typical -OH signals in the presence of surfactants. The 3250 cm^{-1} peak is the signature of the strongly hydrogen bonded water population oriented by the electric field of the charged film, known as the $\chi^{(3)}$ effect.[19-21] The water population leading to 3440 cm^{-1} peak has weaker hydrogen bonding, is possibly closer to the surface, and might contain water molecules coordinating to the GO films, though this signal is also affected by the surface electric field.

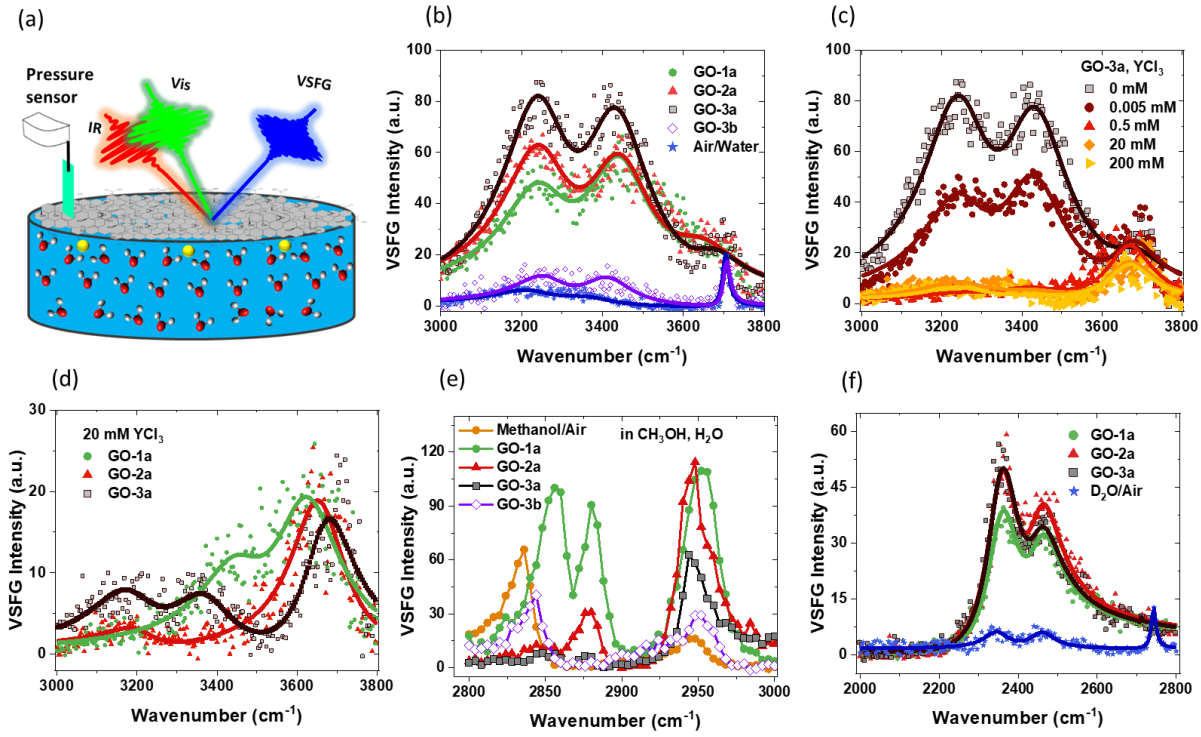

Figure 2. (a) Schematic showing the VSFG experiments on the GO/aqueous interface. The yellow spheres represent the adsorption of Y^{3+} ions on the GO surface. (b) VSFG intensity of -OH region of different GO films compared to a bare air/water interface. (c) VSFG intensity of the -OH region of GO-3a films on YCl_3 subphases with varied concentrations. (d) -OH region of VSFG signal for GO-1a, GO-2a, and GO-3a films on 20 mM YCl_3 (e) VSFG intensities of -CH region for various GO films and a bare air/methanol interface. (f) VSFG intensity of the -OD region for different GO

films compared to a bare air/D_2O interface. Here, the GO is suspended in a 1:5 mixture of D_2O and deuterated methanol (CD_3OD).

GO-3a has the strongest VSFG signal likely because it has more functional groups per carbon-carbon bond and these groups lead to a stronger electric field. This is supported by the XPS results (Figure SI1). GO-1a and GO-2a have similar VSFG signals but GO-2a has slightly stronger 3250 cm^{-1} peak, thus agreeing with the supplier information that it is carboxyl-enriched. However, GO-2a still has fewer carboxyl groups compared to GO-3a. It is interesting that the surface pressure for GO-1a was the highest although it has the lowest VSFG signal. The -CH region VSFG data (Figure 2e) suggest that GO-1a has extra hydrocarbon impurities, i.e. oxidative debris, responsible for the higher surface pressure.

The 3640 cm^{-1} (Figure 2b) peak is too high of a frequency to be a water-water hydrogen bond and is likely from the water population trapped in between the GO layers. Earlier VSFG studies by Carr et al.[18] and Hong et al.[11] at the air/water interface did not observe this 3640 cm^{-1} peak so clearly. Ab-initio molecular dynamics (AIMD) studies by David et al. suggest that this peak appears when C/O ratio is low (~ 2) and disappears when it is high (~4).[8] They also did VSFG experiments with spin-coated GO and reduced-GO films on sapphire to compare. However, the sapphire substrate also had a strong peak around 3640 cm^{-1} obscuring the results. Considering that C/O ratio is less than 2 for all samples in this study it is reasonable to say that the present results support that suggestion. However, C/O ratio was ~ 5 and ~ 2 in Carr et al. and Hong et al. studies, respectively. The absence of 3640 cm^{-1} peak may be explained by C/O ratio for the former but not for the latter. This work suggests that C/O ratio is not the only factor, but the film quality also plays a role in the observation of this peak. The films created using the new spreading method are

more uniform and of higher quality, which makes it much easier to detect this distinct water population.

The high quality GO films also allow consideration of ion adsorption, which is directly relevant to membrane applications where the GO film will be saturated with adsorbed ions and water is expected to behave differently. Figure 2c shows VSFG signal from the -OH region as a function of the subphase YCl_3 concentration. As ions adsorb to the GO film, the VSFG signal should decrease, since the adsorbed ions disrupt water organization and screen the charge of the film.[22-24] Above 0.5 mM YCl_3, the 3250 and 3440 cm^{-1} peaks decrease significantly but 3640 cm^{-1} peak stays unchanged, which supports the hypothesis that this signal originates from water molecules in between the GO layers and is thus minimally affected by the adsorbed ions and the diminishing electric field. At 20 mM, GO-3a still has some 3250 and 3440 cm^{-1} signal, probably due to functional groups that are inaccessible to adsorbed ions but can create a local electric field (zoomed in version is shown in Figure SI4). GO-1a and GO-2a samples show a similar trend (data not shown).

VSFG data for GO films created on concentrated subphases relevant to GO membrane applications are shown in Figure 2d. All samples show very similar 3640 cm^{-1} signal, which suggests that the preparation method presented creates similar films even though the GO solutions were obtained from different vendors. The 3250 and 3440 cm^{-1} peaks are clearly different between the samples. These peaks are mostly absent in GO-2a, consistent with the XPS and previous VSFG results that suggest GO-2a has fewer functional groups per C-C bond. GO-3a retains the strongest signal, which supports the prior interpretation that some functional groups may be inaccessible to ions but their local interactions with water molecules can cause the VSFG signal via orientational ordering of water molecules. Understanding the true origin of these differences requires more

detailed investigations. The goal of this work is to demonstrate a simple and efficient method to create high quality GO films. The improved film quality allows detection of subtle differences that can later be compared to computational studies and correlated with membrane applications.

VSFG is a vibrational spectroscopy and can provide information about interfacial chemical signatures.[25] The measurements studying free methanol/air interface and GO films prepared in methanol show that no methanol is present at the interface for the high quality films (Figure 2e). However, the low quality film shows signature of methanol (Figure 2e), possibly due to the large volume of the spreading solution (1 mL). These data show the importance of preparing high quality films with a minimum volume of spreading solution.

The -OH region of VSFG signal may have contributions from -OH groups on GO film. To clarify, GO samples in deuterated methanol were prepared with and spread on D_2O. The results show that there is no detectable -OH signal from GO films under these conditions (Figure SI-3a). However, the VSFG -OD region (Figure 2f) shows interesting differences compared to -OH region (Figure 2b). First, the expected high frequency peak around 2700 cm^{-1}, i.e. the deuterated 3640 cm^{-1} peak analogue, is completely missing. Second, the VSFG intensity of GO-2a and GO-3a are more similar in contrast to -OH region, where the GO-3a VSFG signal is significantly higher. These results broadly suggest that D_2O and H_2O interact differently with GO films. Indeed, recent studies demonstrated that GO membranes can be used for isotopic water separations.[26, 27] The high quality films prepared in this study allow one to observe clear differences between the interactions of D_2O and H_2O with GO, which provides new opportunities to understand the fundamental interactions underlying isotopic water selectivity of GO.

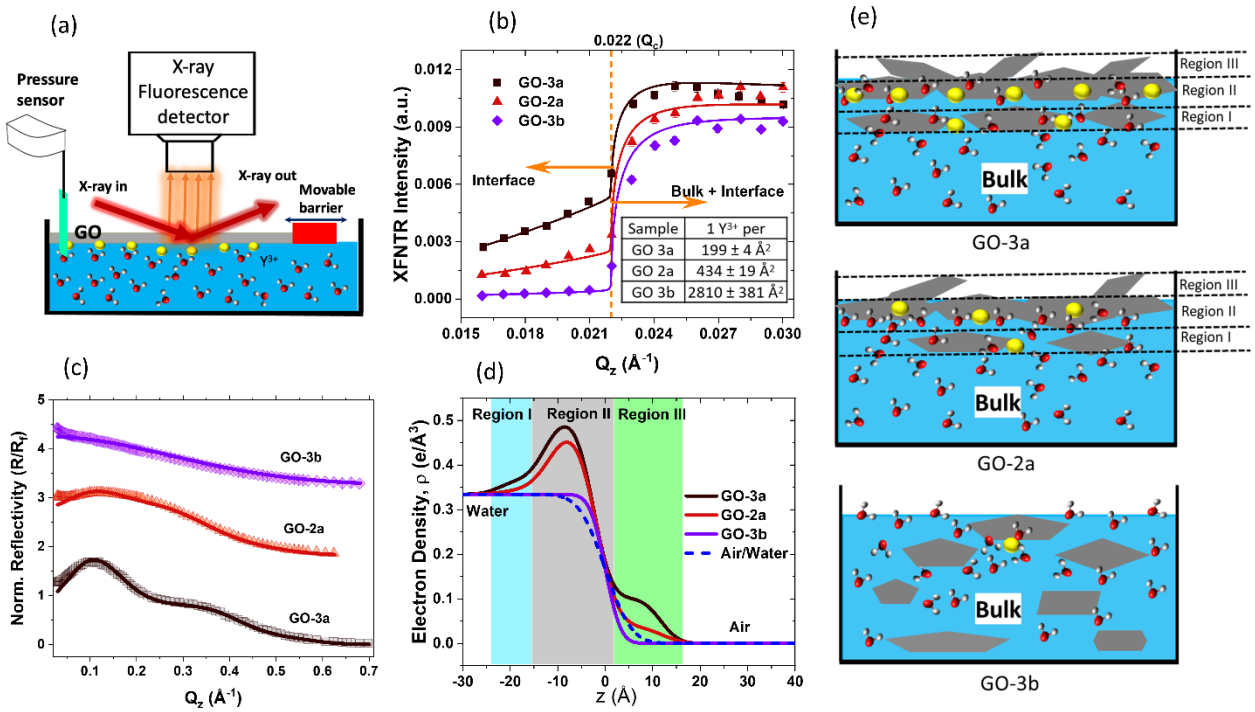

Figure 3. (a) Schematic showing X-ray fluorescence near total reflection (XFNTR) and X-ray reflectivity (XR) measurements of GO films at air/aqueous interface. The GO films were compressed to 20 mN/m, except for GO-3b which reached a maximum surface pressure of 4 mN/m. The yellow spheres represent the adsorption of Y^{3+} ions on the GO surface. (b) XFNTR intensity plotted over momentum transfer Q_Z for different GO films each prepared on a 0.5 mM YCl_3 subphase. Error bars are derived from experimental counting statistics. Inset table shows the density of Y^{3+} ions adsorbed to the GO films obtained by fitting the XFNTR data. (c) Normalized XR intensity plotted over momentum transfer Q_Z for different GO films. The data are vertically offset for clarity. (d) Calculated electron density profile as a function of distance from the interface (Z) for different GO films prepared on 0.5 mM YCl_3 subphases compared to the electron density profile of an ideal air/water interface without GO. (e) Cartoons showing possible adsorption of Y^{3+} ions on GO films with different structures.

While VSFG gives direct information about the interfacial water structure, it only gives indirect information on the film structure and ion adsorption. To obtain direct information about the film and ion adsorption, synchrotron X-ray reflectivity (XR) and X-ray fluorescence near total reflection (XFNTR) experiments were conducted at Sector 15 ID-C of Advanced Photon Source (Figure 3).[28, 29]

XFNTR can directly quantify the number of adsorbed ions at the interface.[28] The element-specific fluorescence emission signal of Y ($K_{\alpha 1}$, 14.958 keV) was recorded as a function of the incidence angle below and above the critical angle (Figure 3a, b). Because the refractive index of water for X-rays is less than 1, X-rays undergo total external reflection below the critical angle (Q_C). Only the evanescent waves penetrate a few nanometers near the interface, which allows quantification of the total number of yttrium ions in this region. Fluorescence signal measured at $Q_Z < Q_C$ is generated by ions at the interface while signal measured at Q_Z greater than the critical angle stems from ions at the interface and in the bulk. Quantitative fitting of the XFNTR data for GO-3a and GO-2a films on 0.5 mM YCl_3 subphases give coverages of 1 Y^{3+} ion per 199 ± 4 Å^2 and 434 ± 19 Å^2, respectively.[28] These results broadly agree with VSFG and XPS results discussed before, which show that GO-3a has higher surface charge and more carboxyl groups per carbon-carbon bond. The number of carboxyl groups is not the only factor in ion adsorption, as not all functional groups may be available to interact with the subphase due to the structural organization of the GO film or ions may adsorb on other defect sites or functional groups.

To understand the interfacial film structure, XR experiments were conducted. XR records the specularly reflected X-ray intensity from the air/water interface as a function of the incident angle θ, which is related to the vertical momentum transfer via $Q_z = \frac{4\pi}{\lambda} sin\left(\frac{2\theta}{2}\right)$. Figure 3c shows the XR data, and the electron density profiles derived from them are shown in Figure 3d, which

were calculated using a Parratt formalism.[28, 30] A three-layer model is necessary to fit GO-3a data, which shows clear oscillations due to the layered structure of the film (Figure 3c). The oscillations are less pronounced for GO-2a, which suggests a lower electron density contrast or a lower quality film. The obtained fit parameters are given in the Table SI5. It is important to note that in a lower resolution experiment these three layers may appear as a single layer.

Both GO-2a and GO-3a have a 1.5 nm main layer, labeled Region II in Figure 3d and e. Considering that a hydrated GO layer is approximately 1 nm thick, this core region likely consists of 1-2 layers. There is also additional material below and above this main layer, labelled as Regions I and III, respectively. These regions may be due to tilted GO flakes or extra GO layers. In GO-3a, the electron density of these extra layers is significantly higher compared to the corresponding layers in GO-2a. There may be several reasons for this. First, there is more Lu^{3+} adsorption on GO-3a, which increases the overall electron density and XR intensity. As shown above with VSFG and the surface pressure measurements, there is more oxidative debris in GO-2a, which likely dilutes the real GO flake density in the film. XR data support those results and show that GO-3a possibly has thicker, multilayer GO flakes on average compared to GO-2a. Finally, the low quality GO-3b sample did not form a distinguishable film, as expected (Figure 3 c-e).

In summary, this paper reported a simple but effective method to prepare ultra-thin GO films at the air/water interface and compared GO films created from dispersions obtained from three different vendors. The high quality films at the air/water interface, free from substrate effects, allowed clear observation of nanoscale differences between the films. This method paves the way for future studies to elucidate the complex separation mechanisms underpinning GO membrane success. Three water bands were observed in VSFG experiments and have two different origins. The 3250 and 3440 cm^{-1} bands are due to water alignment generated from the surface charge of

the GO film while the 3640 cm^{-1} peak is from water molecules that are directly coordinated to the GO film. This high frequency peak, which appears to be insensitive to ion adsorption, was not clearly observed in previous studies[11, 18] but predicted in AIMD studies.[8] The higher quality ultra-thin films created here facilitated observation of this water population. Interestingly, this peak cannot be observed in D_2O experiments, which provides important insights for future isotope separations studies. Additional XR data revealed the structure of the high quality prepared films and XFNTR data demonstrate improved trivalent ion adsorption for the high quality films. These experiments provide a consistent method to create GO films at the air/water interface, which can be utilized in a variety of future investigations. Finally, the complementary use of X-ray and VSFG experiments in a single study provided a detailed picture, which cannot be obtained by a single method.[31-33]

ASSOCIATED CONTENT

Supporting Information. Experimental details of SFG and synchrotron experiments, XPS characterization of GO films, additional SFG data on D_2O subphase, zoomed in version of Figure 2c, and fit parameters of SFG and XR data analysis.

AUTHOR INFORMATION

Corresponding Author

*AU, Email: ahmet@anl.gov, Web: www.anl.gov/profile/ahmet-uysal

Author Contributions

The manuscript was written through contributions of all authors. All authors have given approval to the final version of the manuscript.

Notes

The authors declare no competing interest.

ACKNOWLEDGMENT

We thank Wei Bu for helping with synchrotron experiments, Xiao-Min Lin for helping with CNM experiments, and Jiaxing Huang for providing GO samples for preliminary studies and useful discussions. This work was supported by the U.S. Department of Energy, Office of Science, Office of Basic Energy Sciences, Division of Chemical Sciences, Geosciences, and Biosciences, Early Career Research Program, under contract DE-AC02-06CH11357. Use of the Advanced Photon Source and the Center for Nanoscale Materials, both Office of Science User Facilities operated for the U.S. Department of Energy (DOE) Office of Science by Argonne National Laboratory, was supported by the U.S. DOE under Contract No. DE-AC02-06CH11357. NSF's ChemMatCARS Sector 15 is principally supported by the Divisions of Chemistry (CHE) and Materials Research (DMR), National Science Foundation, under Grant NSF/CHE-1834750. This work made use of the Keck-II facility of Northwestern University's NUANCE Center, which has received support from the SHyNE Resource (NSF ECCS-2025633), the IIN, and Northwestern's MRSEC program (NSF DMR-1720139).

REFERENCES

1. Mi, B., Graphene Oxide Membranes for Ionic and Molecular Sieving. *Science* **2014,** *343* (6172), 740-742.

2. Joshi, R. K.; Carbone, P.; Wang, F. C.; Kravets, V. G.; Su, Y.; Grigorieva, I. V.; Wu, H. A.; Geim, A. K.; Nair, R. R., Precise and Ultrafast Molecular Sieving Through Graphene Oxide Membranes. *Science* **2014,** *343* (6172), 752-754.

3. Yang, Q.; Su, Y.; Chi, C.; Cherian, C. T.; Huang, K.; Kravets, V. G.; Wang, F. C.; Zhang, J. C.; Pratt, A.; Grigorenko, A. N.; Guinea, F.; Geim, A. K.; Nair, R. R., Ultrathin graphene-based membrane with precise molecular sieving and ultrafast solvent permeation. *Nature Materials* **2017,** *16* (12), 1198-1202.

4. Xue, S.; Ji, C.; Kowal, M. D.; Molas, J. C.; Lin, C.-W.; McVerry, B. T.; Turner, C. L.; Mak, W. H.; Anderson, M.; Muni, M., Nanostructured graphene oxide composite membranes with ultrapermeability and mechanical robustness. *Nano Letters* **2020,** *20* (4), 2209-2218.

5. Thamaraiselvan, C.; Wang, J.; James, D. K.; Narkhede, P.; Singh, S. P.; Jassby, D.; Tour, J. M.; Arnusch, C. J., Laser-induced graphene and carbon nanotubes as conductive carbon-based materials in environmental technology. *Materials Today* **2020,** *34*, 115-131.

6. Foller, T.; Madauß, L.; Ji, D.; Ren, X.; De Silva, K. K. H.; Musso, T.; Yoshimura, M.; Lebius, H.; Benyagoub, A.; Kumar, P. V.; Schleberger, M.; Joshi, R., Mass Transport via In-Plane Nanopores in Graphene Oxide Membranes. *Nano Letters* **2022,** *22* (12), 4941-4948.

7. Tan, S.; Zhang, D.; Nguyen, M.-T.; Shutthanandan, V.; Varga, T.; Rousseau, R.; Johnson, G. E.; Glezakou, V.-A.; Prabhakaran, V., Tuning the Charge and Hydrophobicity of Graphene Oxide Membranes by Functionalization with Ionic Liquids at Epoxide Sites. *ACS Appl. Mater. Interfaces* **2022,** *14* (16), 19031-19042.

8. David, R.; Tuladhar, A.; Zhang, L.; Arges, C.; Kumar, R., Effect of Oxidation Level on the Interfacial Water at the Graphene Oxide–Water Interface: From Spectroscopic Signatures to Hydrogen-Bonding Environment. *J. Phys. Chem. B* **2020,** *124* (37), 8167-8178.

9. Cote, L. J.; Kim, F.; Huang, J., Langmuir−Blodgett Assembly of Graphite Oxide Single Layers. *J. Am. Chem. Soc.* **2009,** *131* (3), 1043-1049.

10. Kim, J.; Cote, L. J.; Kim, F.; Yuan, W.; Shull, K. R.; Huang, J., Graphene Oxide Sheets at Interfaces. *J. Am. Chem. Soc.* **2010,** *132* (23), 8180-8186.

11. Hong, Y.; He, J.; Zhang, C.; Wang, X., Probing the Structure of Water at the Interface with Graphene Oxide Using Sum Frequency Generation Vibrational Spectroscopy. *J. Phys. Chem. C* **2022,** *126* (3), 1471-1480.

12. Valtierrez-Gaytan, C.; Ismail, I.; Macosko, C.; Stottrup, B. L., Interfacial activity of graphene oxide: Anisotropy, loading efficiency and pH-tunability. *Colloids and Surfaces A: Physicochemical and Engineering Aspects* **2017,** *529*, 434-442.

13. Bonatout, N.; Muller, F.; Fontaine, P.; Gascon, I.; Konovalov, O.; Goldmann, M., How exfoliated graphene oxide nanosheets organize at the water interface: evidence for a spontaneous bilayer self-assembly. *Nanoscale* **2017,** *9* (34), 12543-12548.

14. McCoy, T. M.; Armstrong, A. J.; Moore, J. E.; Holt, S. A.; Tabor, R. F.; Routh, A. F., Spontaneous surface adsorption of aqueous graphene oxide by synergy with surfactants. *Phys. Chem. Chem. Phys.* **2022,** *24* (2), 797-806.

15. Kim, F.; Cote, L. J.; Huang, J., Graphene oxide: surface activity and two-dimensional assembly. *Advanced Materials* **2010,** *22* (17), 1954-1958.

16. Nie, H.-L.; Dou, X.; Tang, Z.; Jang, H. D.; Huang, J., High-yield spreading of water-miscible solvents on water for Langmuir–Blodgett assembly. *J. Am. Chem. Soc.* **2015,** *137* (33), 10683-10688.

17. López-Díaz, D.; Merchán, M. D.; Velázquez, M. M.; Maestro, A., Understanding the Role of Oxidative Debris on the Structure of Graphene Oxide Films at the Air–Water Interface: A Neutron Reflectivity Study. *ACS Appl. Mater. Interfaces* **2020,** *12* (22), 25453-25463.

18. Carr, A. J.; Kumal, R. R.; Bu, W.; Uysal, A., Effects of ion adsorption on graphene oxide films and interfacial water structure: A molecular-scale description. *Carbon* **2022,** *195*, 131-140.

19. Chen, X.; Hua, W.; Huang, Z.; Allen, H. C., Interfacial Water Structure Associated with Phospholipid Membranes Studied by Phase-Sensitive Vibrational Sum Frequency Generation Spectroscopy. *J. Am. Chem. Soc.* **2010,** *132* (32), 11336-11342.

20. Tuladhar, A.; Piontek, S. M.; Frazer, L.; Borguet, E., Effect of Halide Anions on the Structure and Dynamics of Water Next to an Alumina (0001) Surface. *J. Phys. Chem. C* **2018,** *122* (24), 12819-12830.

21. Ohno, P. E.; Wang, H.-f.; Geiger, F. M., Second-order spectral lineshapes from charged interfaces. *Nature Communications* **2017,** *8* (1), 1032.

22. Kumal, R. R.; Nayak, S.; Bu, W.; Uysal, A., Chemical Potential Driven Reorganization of Anions between Stern and Diffuse Layers at the Air/Water Interface. *J. Phys. Chem. C* **2021**.

23. Jena, K. C.; Covert, P. A.; Hore, D. K., The Effect of Salt on the Water Structure at a Charged Solid Surface: Differentiating Second- and Third-order Nonlinear Contributions. *J. Phys. Chem. Lett.* **2011,** *2* (9), 1056-1061.

24. Rehl, B.; Gibbs, J. M., Role of Ions on the Surface-Bound Water Structure at the Silica/Water Interface: Identifying the Spectral Signature of Stability. *J. Phys. Chem. Lett.* **2021,** *12* (11), 2854-2864.

25. Johnson, C. M.; Baldelli, S., Vibrational Sum Frequency Spectroscopy Studies of the Influence of Solutes and Phospholipids at Vapor/Water Interfaces Relevant to Biological and Environmental Systems. *Chemical Reviews* **2014,** *114* (17), 8416-8446.

26. Mohammadi, A.; Daymond, M. R.; Docoslis, A., New insights into the structure and chemical reduction of graphene oxide membranes for use in isotopic water separations. *Journal of Membrane Science* **2022**, 120785.

27. Ching, K.; Baker, A.; Tanaka, R.; Zhao, T.; Su, Z.; Ruoff, R. S.; Zhao, C.; Chen, X., Liquid-phase water isotope separation using graphene-oxide membranes. *Carbon* **2022,** *186*, 344-354.

28. Bera, M. K.; Bu, W.; Uysal, A., Liquid Surface X-Ray Scattering. In *Physical Chemistry of Gas-Liquid Interfaces*, Elsevier: 2018; pp 167-194.

29. Pershan, P. S.; Schlossman, M., *Liquid surfaces and interfaces: synchrotron x-ray methods*. Cambridge University Press: 2012.

30. Danauskas, S. M.; Li, D.; Meron, M.; Lin, B.; Lee, K. Y. C., Stochastic fitting of specular X-ray reflectivity data using StochFit. *Journal of Applied Crystallography* **2008,** *41* (6), 1187-1193.

31. Horowitz, Y.; Steinrück, H.-G.; Han, H.-L.; Cao, C.; Abate, I. I.; Tsao, Y.; Toney, M. F.; Somorjai, G. A., Fluoroethylene Carbonate Induces Ordered Electrolyte Interface on Silicon and Sapphire Surfaces as Revealed by Sum Frequency Generation Vibrational Spectroscopy and X-ray Reflectivity. *Nano Letters* **2018,** *18* (3), 2105-2111.

32. Nayak, S.; Kumal, R. R.; Liu, Z.; Qiao, B.; Clark, A. E.; Uysal, A., Origins of Clustering of Metalate–Extractant Complexes in Liquid–Liquid Extraction. *ACS Appl. Mater. Interfaces* **2021,** *13* (20), 24194-24206.

33. Sung, W.; Wang, W.; Lee, J.; Vaknin, D.; Kim, D., Specificity and Variation of Length Scale over Which Monovalent Halide Ions Neutralize a Charged Interface. *J. Phys. Chem. C* **2015,** *119* (13), 7130-7137.